Physics of semiconductor devices & renewable energies journal

Vol. 03 n. 01 (2026) ;
Journal homepage: www.psdrej.net

Fluid Modeling Study on The Effects of Argon Addition to Oxygen for Ozone Generation

Nesrine Labdouni, Djilali Benyoucef and Hocine Tebani

Department of Technology, University of Hassiba Ben Bouali University of Hassiba Ben Bouali

*Corresponding author*Email:* n.labdouni@univ-chlef.dz

Abstract
The present investigation uses a chemical and computational model based on a discharge electrical insulator barrier in O_2-Ar mixtures at the pressure of air to evaluate the crucial impact that the distribution pattern of this gas mixture plays in the plasma discharge. A 6 kV sinusoidal voltage applied at a frequency of 3 kHz drives the discharge, which is generated by two dielectrics with a relative permittivity of 9.96. We decide to simulate with one-dimensional geometry and the physics-based kinetic methods that are part of the COMSOL Multiphysics software. Ozone is produced via fundamental chemical processes that are analyzed. The findings showed the current, voltage, and density of both freshly created and pre-existing species.

Keywords: *Index Terms - Ozone, Plasma, Argon, Dielectric Barrier Discharge, Fluid Model, Atmospheric Pressure.*

I. INTRODUCTION

Ozone is well recognized as a significant oxidizing agent that finds usage in a variety of industrial applications, including the disinfection of water and atmospheric air, as a result of growing environmental protection concerns [1]. In comparison to oxygen, it is a very reactive and changeable gas made up of three oxygen atoms. Ozone may be created using a dielectric boundary discharge (DBD) generator [2].
Dielectric-barrier discharges (DBD) or barrier discharges are other names for silent discharges [3], have crucial benefits in plasma chemistry and surface processing. Usually operating at atmospheric pressure, it is a discharge that uses low temperatures. Generally, two parallel electrodes spaced a few millimeters apart by a dielectric layer are used to create DBD plasma. Which are powered by an alternating current (Ac) voltage that has a frequency between 10 Hz and 100 kHz. Glass, quartz, ceramics, or polymer coating can all be used to create the dielectric barrier.
Applications of plasma technology are highly attractive, especially in the areas of ozone production, polymer surface alteration, carbon dioxide laser excitation, pollution control, plasma chemical gas accumulation, and excimer lamps, plasma-display panels, and medical fields such as disinfection [4–7, 8]. Meanwhile, several scientists have discovered diffuse plasmas in different

atmospheric-pressure gases' boundary discharges, such as Oxygen [9] and mixture Argon-Oxygen [10], Oxygen-nitrogen [11], argon [12] or nitrogen [13].
A thorough knowledge of the chemistry and physics of plasma and discharge is necessary for the creation of a new method that utilizes this discharge. Since knowledge of different gas mixtures are used to perform chemical processes in barrier discharge plasma is necessary for the development of industrial reactors, there is now a lot of study being done on these procedures [14]. We have selected two gas mixture of O_2 and Ar to study the chemical efficiency and physical characteristics of barrier discharges.
A significant chemical process was present in the plasma produced in the DBD discharge in O_2-Ar, where there is a formation of active species by collision of electrons with the Oxygen and Argon molecules. The process and spatiotemporal features of macroscopic plasma amounts of non-thermal gas discharge at low pressures may still be efficiently investigated using numerical modeling [15].
This paper analyzes the spatiotemporal distribution of electrons and other species in the plasma by simulating atmospheric pressure dielectric barrier discharge in O_2-Ar mixtures using COMSOL Multiphysics, which is based on a fluid model.

II. NUMERICAL MODEL

In order to quickly calculate discharge current, voltage, electron density, electron temperature, and other macroscopic features, COMSOL Multiphysics provides a fluid model for simulation that solves continuity, momentum, and energy equations and combines them with Poisson's equation. From [16], we obtain the following equations:

A. Electron Transport

The electron density's continuity model is established using:

$$\frac{\partial n_e}{\partial t} + \nabla.\Gamma_e = R_e \quad (1)$$

$$\Gamma_e = -\mu_e E n_e - \nabla\left(D_e n_e\right) \quad (2)$$

Were

n_e : Density of electron $\left(1/m^3\right)$

R_e : Assess the expression of electrons. $\left(1/m^3.s\right)$

μ_e : Electron mobility $\left(m^2/V.s\right)$

E : Electric field $\left(V/s\right)$

D_e : Diffusion coefficient of electron $\left(m^2/s\right)$

e : Electron.

Electron energy is defined via:

$$\frac{\partial n_\varepsilon}{\partial t} + \nabla.\Gamma_\varepsilon + E.\Gamma_e = R_\varepsilon \quad (3)$$

$$\Gamma_\varepsilon = -\mu_\varepsilon E n_\varepsilon - \nabla\left(D_\varepsilon n_\varepsilon\right) \quad (4)$$

With:

n_ε : Electron's energy density $\left(\mathrm{V/m^3}\right)$

R_ε : Energy loss or gain due to inelastic collisions $\left(\mathrm{V/(m^3.}s)\right)$

μ_ε : Mobility of electron energy $\left(m^2/\mathrm{V}.s\right)$

D_ε : Energy diffusivity of electron $\left(m^2/s\right)$

ε : Energy.

The energy of an electron, $\varepsilon(V)$ calculated by:

$$\varepsilon = \frac{n_\varepsilon}{n_e} \tag{5}$$

Rate coefficients or Townsend coefficients are used to indicate the coefficients that originate from the above equations, depending on the system's molar concentration.

Assume that exist P collisions between inelastic electrons and neutrals and M processes that influence the increase or decrease of electron density.

The collisional energy loss throughout all processes is added together to determine the electron energy loss:

$$R_e = \sum_{j=1}^{p} x_j k_j N_n n_e \Delta\varepsilon_j \tag{6}$$

Where:

p : collisions between inelastic electrons and neutrals;

x_j : The mole fraction of the target species for the reaction. j ;

k_j : Reaction rate coefficient $j\left(m^3/s\right)$;

N_n : Density of total neutral numbers $\left(1/m^3\right)$;

$\Delta\varepsilon_j$: Reaction-related energy loss $j(V)$

The mean electron energy ε has an exponential relationship with the Townsend coefficients k_j. A function of the following kind can be used to fit the Townsend coefficients when a Maxwellian EEDF is assumed:

$$k_j = A\varepsilon^\beta e^{-E/\varepsilon} \tag{7}$$

B. Electrostatic Equations

. Electrostatic field:

$$-\nabla.\varepsilon_0.\varepsilon_r\nabla V = \rho \tag{8}$$

. he spaces charge density:

$$\rho = q\left(\sum_{k=1}^{N} Z_k n_k - n_e\right) \quad (9)$$

. The constitutive relation:

$$D = \varepsilon_0 \varepsilon_r E \quad (10)$$

Submicroscopic characteristics of the coating medium that has dielectric feature and the relevant material properties are explained by relation (10) by connecting the electric field (E) and electric displacement (D).

The following limiting condition adds to surface charge buildup to borders:

$$-n.\left(D_1 - D_2\right) = \rho_s \quad (11)$$

With

ρ_s is the boundary's solution to the distributed ODE that follows:

$$\frac{d\rho_s}{dt} = n.\mathrm{J}_i + n.\mathrm{J}_e \quad (12)$$

With

$n.\mathrm{J}_i$ and $n.\mathrm{J}_e$ are the wall's total electron current density and total ion current density are both represented by the normal component.

III. CHEMICAL MODEL

The electron collision cross sections with argon and oxygen molecules are taken from reference [17-18] listed in Table I.

TABLE I: DATABASES

Reaction	***Formula***	***Reaction***	***Formula***
1	$e+O^+ \Rightarrow O$	19	$e+O_2 \Rightarrow e+O_2$
2	$e+O_2^+ \Rightarrow O+O$	20	$e+O_2 \Rightarrow e+O_{2a1d}$
3	$e+O_2^+ \Rightarrow O+O_{1d}$	21	$e+O_{2a1d} \Rightarrow e+O_2$
4	$e+O_2^+ \Rightarrow O_{1d}+O_{1d}$	22	$e+O_2 \Rightarrow e+O_{2b1s}$
5	$e+O_2^+ \Rightarrow O_{1d}+O_{1s}$	23	$e+O_{2b1s} \Rightarrow e+O_2$
6	$e+O_3^+ \Rightarrow O+O+O$	24	$e+O_2 \Rightarrow e+O_{245}$
7	$e+O_3^+ \Rightarrow O_2+O$	25	$e+O_{245} \Rightarrow e+O_2$
8	$e+O_4^+ \Rightarrow O_2+O_2$	26	$e+O_2 \Rightarrow e+O+O$
9	$e+O_2+O_2 \Rightarrow O_2^- +O_2$	27	$e+O_2 \Rightarrow e+O+O_{1d}$
10	$e+O+O_2 \Rightarrow O^-+O_2$	28	$e+O_2 \Rightarrow e+O+O_{1s}$
11	$e+O+O_2 \Rightarrow O+O_2^-$	29	$e+O_2 \Rightarrow e+e+O_2^+$
12	$e+O_3+O_2 \Rightarrow O_3^- +O_2$	30	$e+O_2 \Rightarrow e+e+O+O^+$
13	$e+O_3 \Rightarrow e+O_2+O$	31	$e+O^- \Rightarrow 2e+O$
14	$e+O_2 \Rightarrow e+O_2$	32	$e+Ar \Rightarrow e+Ar$
15	$e+O_2 \Rightarrow O+O^-$	33	$e+Ar \Rightarrow e+Ar_s$
16	$e+O_3 \Rightarrow e+O_3$	34	$e+Ar_s \Rightarrow e+Ar$
17	$e+O_3 \Rightarrow O_2^-+O$	35	$e+Ar \Rightarrow 2e+Ar^+$
18	$e+O_3 \Rightarrow 2e+O_3^+$	36	$e+Ar_s \Rightarrow 2e+Ar^+$

The electrons mobility is calculated through the electron's collisions cross sections. However, the ions mobilities are taken from the measured data of Ellis et al. [19].

A Lennard-Jones type interaction potential is taken into consideration when calculating the excited particles' diffusion coefficients [20].
The Arrhenius equation [21] is used to quantitatively determine the rate constant kf for the reactions that are utilized in our model token.

$$k^f = Ae^{E_a/RT} \quad (13)$$

From:
A: The component before the exponential;
T: Temperature (kelvin);
Ea: Reaction's activation energy (measured in the identical units as R*T);
R: The widespread gas constant.

Table II lists the significant reactions that were taken into account in our investigation.

TABLE II: REACTION SET

Reaction	***Formula***	***Rate coefficient***	***Ref***
1	$Ar^+ + O^- \Rightarrow Ar + O$	7.51e-14*(300/T) $^{0.5}$	[22]
2	$Ar^+ + O_2^- \Rightarrow Ar + O_2$	7.51e-14*(300/T) $^{0.5}$	[22]
3	$Ar{+}{+} + O_3^- \Rightarrow Ar + O_3$	7.51e-14*(300/T) $^{0.5}$	[22]
4	$Ar^+ + O_4^- \Rightarrow Ar + 2O_2$	7.51e-14*(300/T) $^{0.5}$	[22]
5	$Ar_s + O_2 \Rightarrow Ar + O + O$	0.46*2.2e-16	[22]
6	$Ar_s + O_2 \Rightarrow Ar + O + O_{1d}$	0.52*2.2e-16	[22]
7	$Ar_s + O_2 \Rightarrow Ar + O + O_{1s}$	0.02*2.2e-16	[22]
8	$Ar_s + O \Rightarrow Ar + O$	4.1e-17	[22]
9	$O + O_2 + Ar \Rightarrow O_3 + Ar$	3.9e-46*(300/T)$^{1.9}$	[23]
10	$O_{2b1s} + Ar \Rightarrow O_2 + Ar$	1.5e-23	[22]
11	$Ar + O_{1d} \Rightarrow Ar + O$	2.0947e-17*exp (-309.4467/T)	[22]
12	$Ar^+ + O_2 \Rightarrow Ar + O_2^+$	6.3e-17*exp(T/300) $^{-0.78}$	[22]
13	$Ar^+ + O \Rightarrow Ar + O^+$	6.4e-18	[22]
14	$O_{1s} + Ar \Rightarrow Ar + O_{1d}$	5e-23	[22]
15	$Ar + 2O \Rightarrow Ar + O_{2a}$	9.85e-41	[22]
16	$O_{2a} + Ar \Rightarrow Ar + O_2$	3e-24*exp(-200/T)	[23]
17	$O_{2b} + Ar \Rightarrow Ar + O_{2a}$	1e-23	[23]
18	$O_4^+ + Ar \Rightarrow Ar + O_2^+ + O_2$	3e-23	[22]
19	$Ar + 2O \Rightarrow Ar + O_2$	4.5e-40*exp(630/T)	[22]
20	$O_{2b} + Ar \Rightarrow O_2 + Ar$	1e-22	[22]
21	$O + Ar \Rightarrow O + Ar$	3e-19	[22]

22	$Ar^{+}+O_{2a}=>Ar+O_2^{+}$	5e-17	[22]
23	$Ar^{+}+O_{2b}=>Ar+O_2^{+}$	5e-17	[22]
24	$Ar+O^{+}<=>Ar^{+}+O$	2.1e-17	[22]
25	$Ar+O_2^{+}<=>Ar^{+}+O_2$	2.1e-17	[22]
26	$Ar+O_{1d}=>Ar+O$	5e-18	[22]
27	$Ar+2O=>Ar+O_2$	$2*2.45e-43*(T)^{-0.63}$	[22]

The following interfacial reactions are implemented in addition to the chemical reactions that were previously utilized. (Table II):

TABLE III: INTERFACIAL REACTION

Reaction	Formula
1	$O^{+}=>O$
2	$O_2^{+}=>O_2$
3	$O_3^{+}=>O_2+O$
4	$O_4^{+}=>O_2+O_2$
5	$O^{-}=>O$
6	$O_2^{-}=>O_2$
7	$O_3^{-}=>O_2+O$
8	$O_4^{-}=>O_2+O_2$
9	$O_{1d}=>O$
10	$O_{1s}=>O$
11	$O_{2a1d}=>O_2$
12	$O_{2b1s}=>O_2$
13	$O=>0.5O_2$
14	$O_3=>O_2+O$
15	$Ar_s=>Ar$
16	$Ar^{+}=>Ar$

IV. RESULTS AND DISCUSSION

When a dielectric barrier discharge occurs under a sinusoidal voltage, the following results are obtained. The reactor is thought of as two 3 cm × 3 cm parallel and plane electrodes that are each covered by a 0.5 mm thick dielectric with a relative permittivity of 9.96. At a pressure of one atmosphere, argon and oxygen gases are pumped into a 1 mm discharge space. The reactor runs at a frequency of 3 kHz with a peak voltage of 6 kV.

Fig. 1. shows the waveforms of the discharge voltage and discharge current as they change over three different time periods. Fig. 2 shows the evolution of particles charges in three periods of

DBD discharge, the abundant ions are O_4^+ O_3^+ O_4^- O_3^-. In fig. 3 we show the evolution of neutrals in three periods of DBD discharge, the abundant neutrals are respectively O_3 which created directly by electrons impact dissociation of oxygen molecule and the metastable O_{2a1d} which created directly by electrons impact excitation.

The primary reasons for the rise in the density of the ions close to the anode are the process of ionization and excitation interactions produced by the electron-molecule impact of argon and oxygen in a strong electric field show Figures 2(a) and (b).

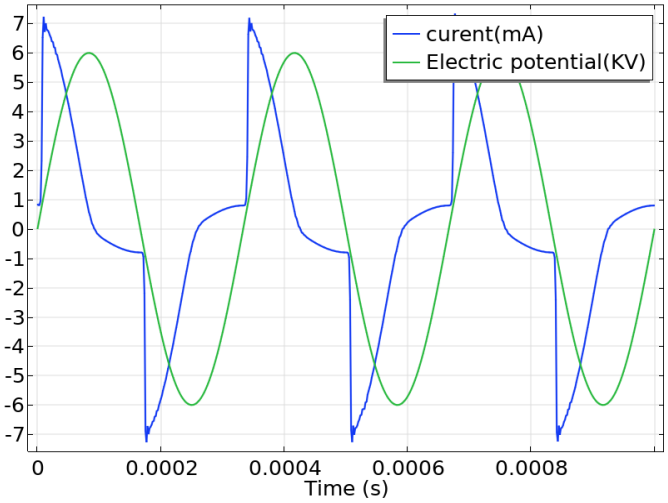
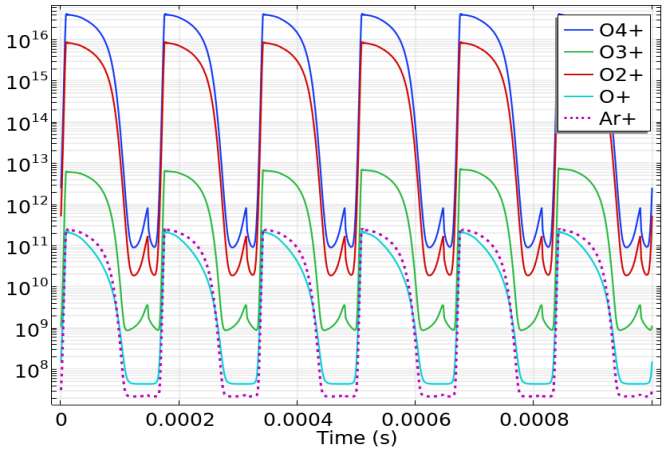
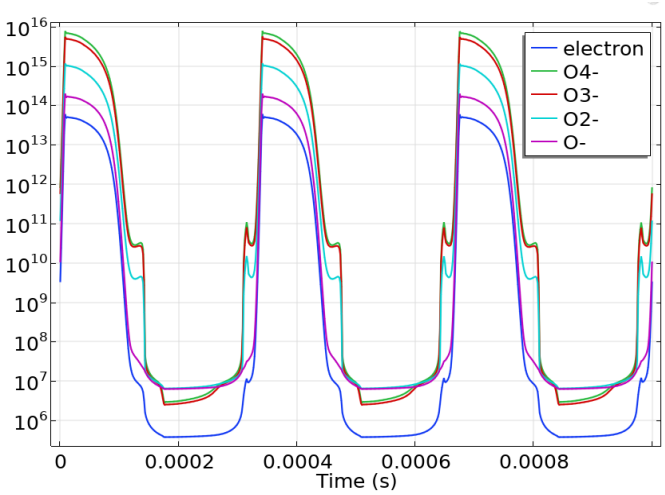


Fig. 1 Voltage-Current characteristic (V–I) in three periods of DBD discharge



(a)



(b)

Fig. 2 Evolution of particles charges densities in m3 unit during three periods of DBD discharge

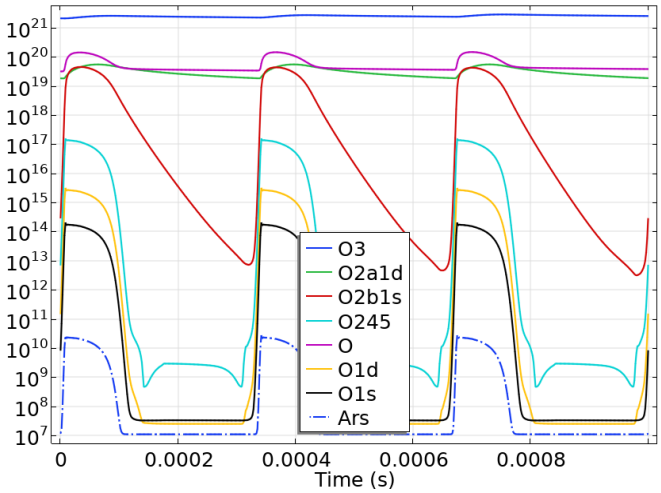


Fig. 3 Evolution of neutrals densities in m3 unit during two periods of DBD discharge

Fig. 3. shows how the presence of argon significantly increased the electron and oxygen ion number densities, which led to the creation of other elements during the discharge, including ozone O_3. Avalanches will continue to develop in this area because the concentration of free electrons and ions is near the dielectric coatings that are related to high voltage. However, a stronger electric field develops between the electrodes as the applied voltage increases, speeding up any free electrons in that area. Uniform avalanches over the gap are the consequence of the electrons gaining enough energy to induce considerable ionization activity due to the high electric field.

V. CONCLUSION

A numerical analysis of DBD's ozone generation in an O_2-Ar mixture provides valuable insights into the plasma chemistry involved, helping to optimize conditions for efficient ozone production.

Such research contributes to the development of sustainable technologies for pollution control and environmental management. The simulation shows that the abundant ions are O_4^+ and O_3^+, it shows also that the abundant neutrals are respectively O_3 and the metastable O_{2a1d}

ACKNOWLEDGMENT

The authors express their gratitude to Algeria's "Ministry of Higher Education and Scientific Research" for funding this study.

REFERENCES

[1] K. Yanallah, F. Pontiga, A. Fernández-Rueda, A. Castellanos. Experimental investigation and numerical modelling of positive corona discharge: Ozone generation. J Phys D Appl Phys. 2009; 42:065202

[2] W.J.M. Samaranayake, Y. Miyahara, T. Namihira, S. Katsuki, R. Hackam, and H. Akiyama, Ozone Production using Pulsed Dielectric Barrier Discharge in Oxygen, IEEE Trans., Dielectrics Electrical Insul., vol. 7, no. 6, pp. 849–854, 2000

[3] U. Kogelschatz, "Dielectric-barrier discharges: Their history, discharge physics and industrial applications," Plasma Chem. Plasma Process. vol. 23, no. 1, pp. 1–46, Mar. 2003.

[4] U. Kogelschatz, Filamentary, patterned, and diffuse barrier discharges, IEEE Trans. Plasma Sci. 30 (2002) 1400.

[5] Zhi Fang, Jinguo Lin, Hao Yang, Yuchang Qiu, "Polyethylene Terephthalate Surface Modification by Filamentary and Homogeneous Dielectric Barrier Discharges in Air" IEEE TRANSACTIONS ON PLASMA SCIENCE, VOL. 37, NO. 5, may 2009.

[6] Zhang, C., Shao, T., Long, K., Yu, Y., Wang, J., Zhang, D., ... & Zhou, Y. (2010). Surface treatment of polyethylene terephthalate films using DBD excited by repetitive unipolar nanosecond pulses in air at atmospheric pressure. IEEE transactions on plasma science, 38(6), 1517-1526.

[7] U. Kogelschatz, "From ozone generators to flat television screens history and future potential of dielectric-barrier discharges ", Pure Appl. Chem. 7 (1999).

[8] M.J. Kirkpatrick, B. Dodet, E. Odic, "Atmospheric Pressure Humid Argon DBD Plasma for the Application of Sterilization -Measurement and Simulation of Hydrogen, Oxygen, and Hydrogen Peroxide Formation", International Journal of Plasma Environment Science & Technology 1, 1 (2007) 96-101.

[9] Benyoucef, D., & Yousfi, M. (2015). Particle modelling of magnetically confined oxygen plasma in low pressure radio frequency discharge. Physics of Plasmas, 22(1).

[10] Baadj, S., Larouci, B., Belasri, A., Pontiga, F., Benmoussa, A., & Saidia, L. (2023). Chemical and Electrical Aspects of Homogeneous Discharge in an Argon-Oxygen Mixture for Ozone Generation. Plasma Medicine, 13(4).

[11] Liu, K., Zheng, Z., Liu, S., & Hu, Y. (2019). Study on the Physical and Chemical Characteristics of DBD: The Effect of N2/O2 Mixture Ratio on the Product Regulation. Plasma Chemistry and Plasma Processing, 39, 1255-1274.

[12] Heneral, A. A., & Avtaeva, S. V. (2020). Atmospheric pressure plasma jets generated by the DBD in argon-air, helium-air, and helium-water vapour mixtures. Journal of Physics D: Applied Physics, 53(19), 195201.

[13] Lahouel, M. H. A., Benyoucef, D., & Tebani, H. (2021). Modeling and parametric study of dielectric barrier discharge in pure nitrogen at atmospheric pressure. Turkish Journal of Physics, 45(1), 26-42.

[14] Kitayama, J. and Kuzumoto, M., Theoretical and Experimental Study on Ozone Generation Characteristics of an Oxygen-Fed Ozone Generator in Silent Discharge, J. Phys. D: Appl. Phys., vol. 30, pp. 2453–2461, 1997.
[15] U. Konelschatz, B. Eliasson and W. Egli, “Dielectric-Barrier Discharges. Principles and Applications” Journal de Physique Iv, Colloque C4, Supplement au Journal de Physique III d'octobre 1997.
[16] M. Ramin. "Two-dimensional simulation of Argon dielectric barrier discharge (DBD) in plasma actuator structure with COMSOL Multiphysics." arXiv preprint arXiv:2304.05698 .2023.

[17] https://nl.lxcat.net/.
[18] BOLSIG+: Electron Boltzmann equation solver. Available from: http://bolsig.laplace.univ-tlse.fr/.

[19] H. W. Ellis, et al., “Transport properties of gaseous ions over a wide energy range,” Atomic data and nuclear data tables, vol. 17, no. 3, pp. 177-210, 1976.

[20] H. Tebani, D. Benyoucef, “A global model for the inductively coupled rf discharges in Ar/H2 mixture,” Przegląd Elektrotechniczny, vol. 97, no.1, pp. 30-36, 2021.

[21] https://www.shodor.org/unchem/advanced/kin/arrhenius.html.

[22] Liu, D., Sun, B., Iza, F., Xu, D., Wang, X., Rong, M., & Kong, M. G. (2017). Main species and chemical pathways in cold atmospheric-pressure Ar+H2O plasmas. Plasma Sources Science and Technology, 26(4), 045009.
[23] Vichiansan, N., Leksakul, K., Chaopaisarn, P., & Boonyawan, D. (2021). Simulation of simple 2D plasma jet model for NO, OH, and H2O2 production via Multiphysics in laminar flow and transport of diluted species through design of experiment method. AIP Advances, 11(3).